Indian Ocean Dipole influence on South American rainfall

Steven C. Chan,[1] Swadhin K. Behera,[2] and Toshio Yamagata[2,3]

Received 2 April 2008; revised 18 May 2008; accepted 16 June 2008; published 19 July 2008.

[1] The rainfall anomalies over South America are found to be influenced by the Indian Ocean Dipole (IOD). Between subtropical La Plata Basin and central Brazil, the IOD excites a dipolar pattern in rainfall anomalies; rainfall is reduced (enhanced) over latter (former) during austral-spring, when IOD reaches its peak phase. A Rossby wave train extends from the subtropical south Indian Ocean to the subtropical South Atlantic. The associated anomaly in surface circulation suggests an intensification of the South Atlantic High. The anomalous anticyclone in the lower troposphere causes anomalous divergence (convergence) of moisture over central Brazil (subtropical La Plata Basin). These results based on the University of Delaware precipitation analysis and the NCEP-NCAR reanalysis data are corroborated by that of the Scale Interaction Experiment-Frontier version 1 (SINTEX-F1) coupled general circulation model. **Citation:** Chan, S. C., S. K. Behera, and T. Yamagata (2008), Indian Ocean Dipole influence on South American rainfall, *Geophys. Res. Lett.*, *35*, L14S12, doi:10.1029/2008GL034204.

1. Introduction

[2] The atmospheric circulation over tropical and subtropical South America in warm seasons has characteristic features of a monsoon system. In the lower troposphere, easterlies from the Atlantic Ocean are veered southward by the Andes as the South American Low-Level Jet (SALLJ) [e.g., *Vera et al.*, 2006]. The SALLJ advects moisture from the Amazon Basin and tropical Atlantic Ocean to subtropical La Plata Basin, where the seasonal rainfall shows two peaks in austral spring and fall. Spring rainfall in La Plata region (Figure 1) is largely determined by transient atmospheric disturbances and SALLJ [e.g., *Nogués-Paegle et al.*, 2002; *Vera et al.*, 2006]. The rainfall in subtropical plains of southeastern South America is found to be influenced by intraseasonal upper tropospheric wave patterns [*Nogués-Paegle and Mo*, 1997], which sometimes originate from the South Pacific [e.g., *Liebmann et al.*, 1999]. On interannual time scales, the subtropical region is shown to be influenced by the El Niño-Southern Oscillation (ENSO) via Pacific-South American Rossby wave trains [e.g., *Mo and Nogués-Paegle*, 2001]. The Antarctic Oscillation is another important source to influence the interannual variability of austral spring precipitation in that region [e.g., *Silvestri and Vera*, 2003].

[1]Department of Meteorology, University of Maryland, College Park, Maryland, USA.
[2]Frontier Research Center for Global Change/JAMSTEC, Yokohama, Japan.
[3]Department of Earth and Planetary Science, University of Tokyo, Tokyo, Japan.

0094-8276/08/2008GL034204

[3] Motivated by the fact that IOD reaches its peak during September-November [e.g., *Saji et al.*, 2005] we investigate in this study its influence on the South America's spring rainfall, which appears similar to a summer-time dipole pattern in atmospheric convection [e.g., *Doyle and Barros*, 2002; *Diaz and Aceituno*, 2003]. The IOD is a coupled climate mode [e.g., *Saji et al.*, 1999; *Yamagata et al.*, 2004] in the Indian Ocean, the positive phase of which (Figure 1c) is associated with warmer (colder) than normal sea surface temperature (SST) off the coast of East Africa (Java-Sumatra). The associated atmospheric teleconnection carries the signal far and wide from the source region [e.g., *Saji and Yamagata*, 2003; *Yamagata et al.*, 2004; *Behera et al.*, 2005].

2. Data and Models

[4] The NCEP-NCAR reanalysis [*Kalnay et al.*, 1996], Hadley Center SST [*Rayner et al.*, 2006] and the University of Delaware gridded precipitation analysis, obtained using the method described by *Willmott and Matsuura* [1995], are used in this study. Besides 42-years of reanalysis and SST data for the period from 1958 to 1999, simulation results from a 200-yr coupled ocean-atmosphere general climate model (CGCM) simulation are used in the analysis to support the statistical significance of the observational findings.

[5] The Scale Interaction Experiment-Frontier version 1 (SINTEX-F1) CGCM is an upgraded version of the SINTEX (Scale Interaction Experiment of EU project) model that is described by *Gualdi et al.* [2003]. The atmosphere model has a T106 spectral representation in the horizontal, and has 19 levels in the vertical. The ocean model OPA8.2, with 31 vertical levels, adopts the Arakawa C grid with a finite mesh in which the meridional grid resolution is about 0.5° in the equatorial region. The SINTEX-F1 has a remarkable skill in reproducing the interannual variability in the Indian and Pacific Oceans [*Luo et al.*, 2003; *Masson et al.*, 2004].

[6] The dynamical interpretation of features in reanalysis data and non-linear CGCM results is not straightforward. Therefore, for further guidance we have used a simple linear barotropic model based on the following vorticity equation.

$$\frac{\partial \xi'}{\partial t} = -\overline{\mathrm{v}}_{\psi}.\nabla \xi' - \mathrm{v}'_{\psi}.\nabla(f + \overline{\xi}) + \mu \nabla^4 \xi' - \lambda \xi' + F \qquad (1)$$

Here terms with overbars are climatological quantities during austral spring, F is the forcing from vorticity stretching/divergent flow, ξ' is vorticity anomaly, v' is rotational vector wind anomaly, μ is the diffusion coefficient (chosen to be 2×10^{16} $\mathrm{m^4 s^{-1}}$), and λ is the Newtonian frictional dissipation coefficient (chosen to be 1/5 $\mathrm{days^{-1}}$). This idealized model with a triangular truncation at T-42 is linearized around the September-

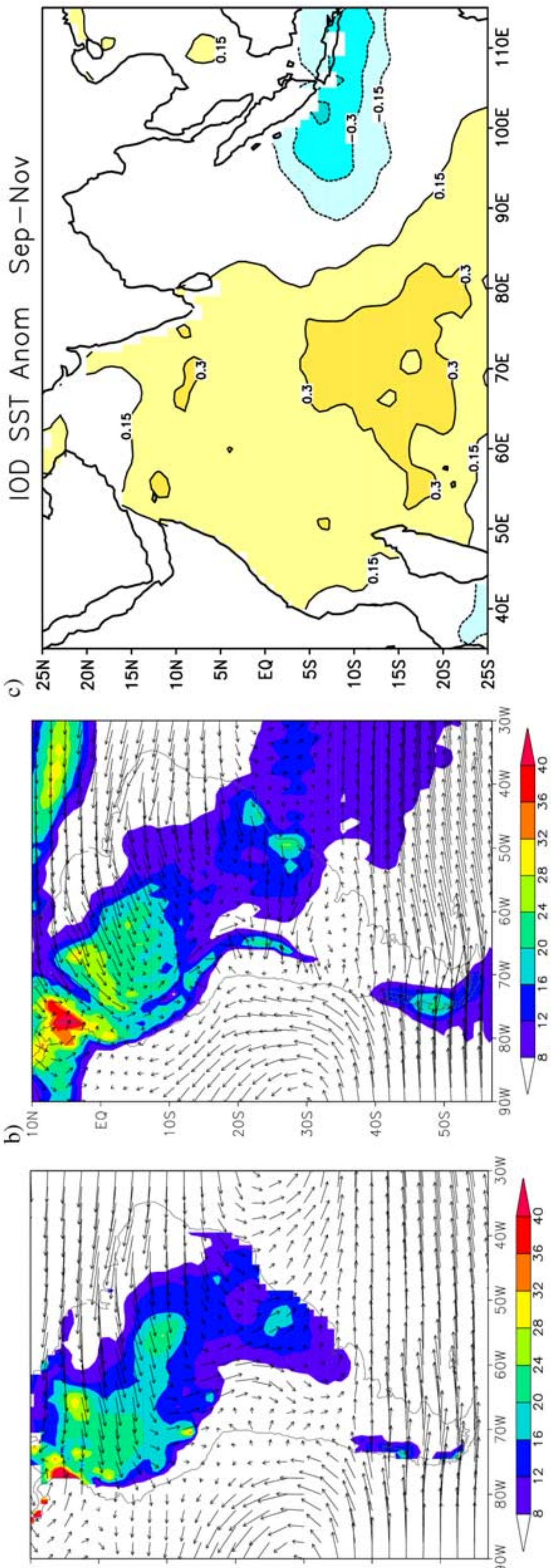

Figure 1. Seasonal climatology of September–November precipitation and 850 hPa wind for (a) observation and (b) SINTEX-F1 results. (c) The September–November composite SST anomalies for 4 pure positive IOD events.

November 200-hPa climatology. The model is then integrated for 20 days using the idealized forcing that would mimic the associated divergence observed during a real IOD event.

3. Composite Analysis

[7] In order to understand IOD's influence on the South American climate, composite rainfall anomalies for positive IOD years are investigated. The positive IOD events are identified by the positive sign of the dipole mode index defined as SST anomaly difference between the western (50°E–70°E, 10°S–10°N) and eastern (90°E–110°E, 10°S-Eq) tropical Indian Ocean [*Saji et al.*, 1999]. The positive IOD events that evolved in non-El Niño years are identified as pure positive IOD events (1961, 1967, 1977, 1994 [after *Yamagata et al.*, 2004]; hereafter referred to as pure IOD events). During these IOD event years, the standard deviation of SST dipole mode index (hereafter referred to as IOD index) is 1.5 or higher for September–November season. The rainfall anomaly composites of pure IOD events show a dipole pattern between the southern and the northern parts of eastern South America (Figure 2a): Precipitation is below normal (above normal) over central Brazil (subtropical La Plata Basin) during austral spring. Southern Chile also receives higher than normal rainfall. The 200-yr record of SINTEX-F1 results, from which 15 pure IOD events are chosen, support those observational features remarkably well (Figure 2b). Unlike positive IOD events, the precipitation patterns during pure negative IOD events are spatially less coherent (not shown).

[8] To further quantify the statistical relation between IOD and South American precipitation, the spatially-averaged index for precipitation anomalies over central Brazil (70°W – 40°W, 25°S – 5°S) is correlated with the IOD index. Because of the interfering influence of IOD and ENSO, partial correlation technique is used to separate the ENSO signal from the IOD signal [e.g., *Saji and Yamagata*, 2003; *Yamagata et al.*, 2004]. The partial correlation coefficient between the IOD index (Niño3) and the central Brazil precipitation index (Figure 2c) is −0.44 (0.18), which is statistically significant (not significant) over the 42 years analysis period at the 95% level using a 2-tailed "t" test. The IOD influence is found to be even higher in the 200-yr SINTEX-F1 results; the corresponding partial correlations for IOD index and Niño3 are −0.54 and −0.12, respectively. An opposite sign is found in the correlation coefficient between IOD index and rainfall anomalies of subtropical La Plata Basin. These results support the composite analyses (Figures 2a and 2b) and indicate a potentially strong relationship between IOD and South American rainfall anomalies.

[9] The negative rainfall anomalies in central Brazil are associated with the 850-hPa anomalous anticyclonic circulation over the South Atlantic, which enhances moisture transport to subtropical La Plata Basin. Rainfall variability in eastern South America is sometimes related to a similar circulation in austral summer [e.g., *Robertson and Mechoso*, 2000]. In the present case, the low-level spring circulation is related to the upper tropospheric anticyclone (Figure 3a) with a region of anomalous ascent to the southwest, which is further discussed in section 4. The anomalous lower

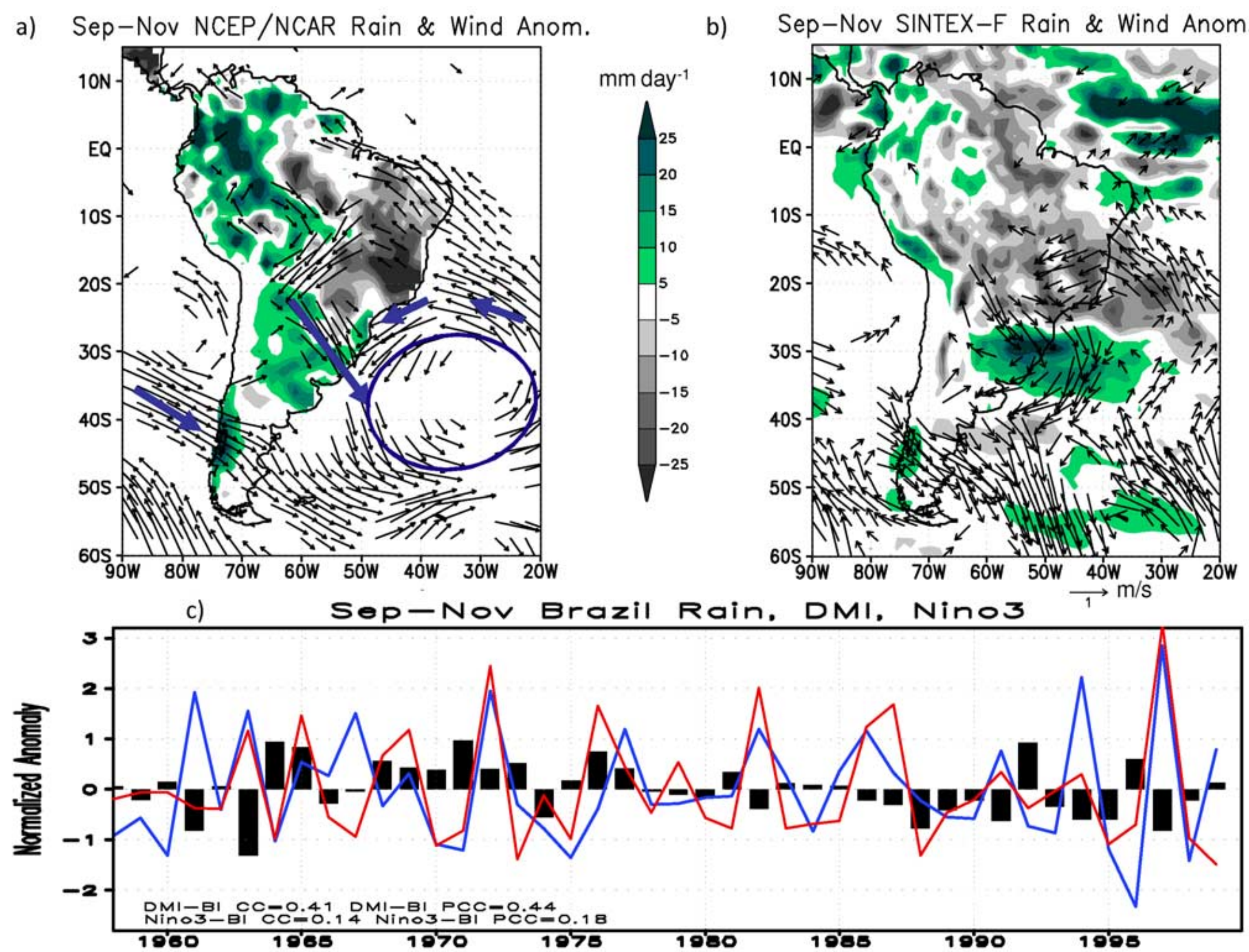

Figure 2. September–November composite of rainfall and 850-hPa wind anomalies during pure positive IOD events for (a) observation and (b) SINTEX-F1 results. Shown values exceed the 95% level of confidence from a t-test. (c) Indices of central Brazil rain (bar), IOD (blue) and Niño3 (red) averaged for September–November.

troposphere anticyclone strengthens the southward or southeastward low-level wind anomalies (compare Figures 1 and 2) between Bolivia and Uruguay. The anomalous convergence of moist air gives rise to anomalous rainfall over the subtropical La Plata Basin. This anomalous convergence is consistent with the Sverdrup balance:

$$\beta v = f\frac{\partial w}{\partial z} \tag{2}$$

The strengthening of low-level northerly wind to the west of the anomalous anticyclone leads to lower troposphere convergence. An anomalous trough along 30°S gives rise to the east-west orientation of the precipitation band in the CGCM composite. On the other hand, the low-level divergence (figure not shown) that is associated with the northward extension (to around 40°W 20°S) of the anomalous anticyclone gives rise to the negative precipitation anomalies over most parts of central and eastern Brazil.

4. Teleconnection

[10] Regional climate anomalies can be caused by teleconnection patterns arising from remote sources that are connected with distant regions via propagating Rossby waves [e.g., *Hoskins and Karoly*, 1981; *Ambrizzi et al.*, 1995; *Trenberth et al.*, 1998]. The Rossby waves are excited in the upper troposphere by the divergent outflow from anomalous deep convection above tropical SST anomalies [*Sardeshmukh and Hoskins*, 1988]. Southern hemisphere teleconnection patterns forced by global wave sources are discussed by *Grimm and Silva Dias* [1995].

[11] In order to understand such atmospheric teleconnections, we made composites of the 200-hPa streamfunction anomalies from the NCEP-NCAR reanalysis and SINTEX-F1 simulation results during pure IOD events (Figures 3a and 3b). In both composites, a wave train originates from the Indian Ocean (similar to that shown by *Saji et al.* [2005]). Those waves produce large streamfunction anomalies over the southern Indian Ocean (Figures 3a and 3b) in response to the Rossby wave source (not shown) that is generated by the IOD divergence/convergence anomalies over the tropical Indian Ocean. The midlatitude waveguide (Figure 3c) then traps the propagating Rossby waves along the stationary Rossby wave paths. The wave train, emanating from the Indian Ocean curves towards the south, propagates to the southern part of South America and then

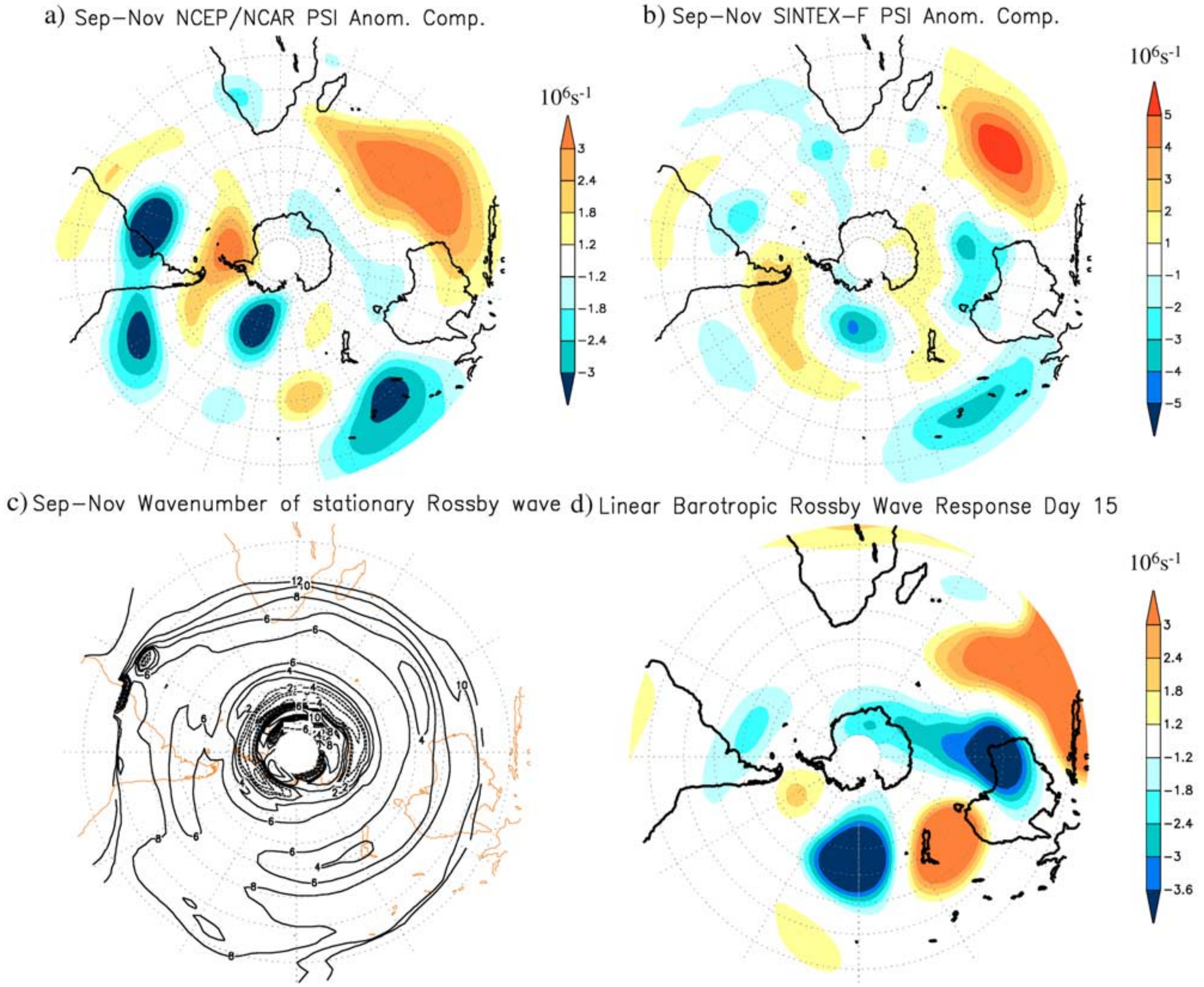

Figure 3. September–November composite of 200 hPa eddy streamfunction anomalies for pure IOD events derived from (a) reanalysis data and (b) SINTEX-F1 results. Values higher than 95% confidence level for a t-test are shown. (c) Wave numbers of stationary Rossby waves for 200-hPa September–November mean condition. (d) Streamfunction after 15 days integration of the linear barotropic model.

turns back to the Indian Ocean via southern Africa. The presence of the double jet in the Southern Hemisphere gives rise to two waveguides. Each jet region contains quite uniform values of stationary Rossby wave numbers bounded meridionally by lower values. Associated with the wave train, there is an upper-tropospheric anomalous anticyclone over central Brazil and adjacent Atlantic Ocean located slightly to the west of the lower-tropospheric anomalous anticyclone (Figures 2a and 2b). The equivalent barotropic structure influences the surface circulation; in particular, it strengthens the SALLJ, which enhances subtropical La Plata Basin rainfall.

[12] This teleconnection emanating from the IOD is further verified from an idealized experiment using a linear barotropic model (equation 1). Similar to the reanalysis and the SINTEX-F1 results, this idealized experiment results also show a wave train (Figure 3d) along the great circle (Figure 3c). The general agreement among anomalous patterns of the idealized model experiment, the reanalysis fields and CGCM data indicates that the teleconnection pattern in the Southern Hemisphere is largely an outcome of the IOD forcing in the tropical Indian Ocean. Some of the dissimilarities seen in the idealized experiment patterns (Figure 3d) indicate the limitation of the simple linear model, which undermines the roles of other processes such as non-linear interactions and adjustments owing to regional air-sea interactions.

5. Conclusion

[13] The NCEP-NCAR reanalysis data and the SINTEX-F1 CGCM results show that the IOD influences the interannual rainfall variability over central Brazil and subtropical La Plata Basin in austral spring. The positive IOD teleconnection manifests as a dipole pattern in the regional rainfall anomalies: Rainfall increases over subtropical La Plata Basin while it decreases over central Brazil. The teleconnection pattern that originates from the southern

Indian Ocean appears as a mid-latitude wave train. The associated low-level anomalous anticyclone found off the coast of Brazil enhances the tropical easterlies and strengthens the SALLJ. The increased moisture flux then gives rise to the anomalously high precipitation over Uruguay and northern Argentina. Conversely, anomalous divergence over eastern and central Brazil suppresses convection and results in decreased precipitation there. An idealized simple model experiment corroborates the teleconnection seen in the reanalysis and CGCM data. It was interesting to verify that the IOD teleconnections also appeared in austral spring of 2006.

[14] The discussion in the present paper focuses on seasonal anomalies. As *Cazes-Boezio et al.* [2003] point out, different intra-seasonal and synoptic disturbances play key roles in the ENSO teleconnection to the La Plata Basin. For realizing the IOD impact on weather systems, the next step is to examine anomalous transient activity in those timescales.

[15] **Acknowledgments.** The authors are thankful to J.-J. Luo and S. Masson for providing the SINTEX-F simulation results. The authors also thank C. R. Mechoso and an anonymous reviewer for their constructive comments and helpful suggestions, which were helpful to improving the quality of the manuscript. SC is thankful to Japan Society for the Promotion of Science and National Science Foundation for funding a summer internship in FRCGC.

References

Ambrizzi, T., B. Hoskins, and H. H. Hsu (1995), Rossby wave propagation and teleconnection patterns in the austral winter, *J. Atmos. Sci.*, *52*, 3661–3672.

Behera, S. K., J.-J. Luo, S. Masson, P. Delecluse, S. Gualdi, A. Navarra, and T. Yamagata (2005), Paramount impact of the Indian Ocean Dipole on the East African short rains: A CGCM study, *J. Clim.*, *18*, 4514–4530.

Cazes-Boezio, G., A. W. Robertson, and C. R. Mechoso (2003), Seasonal dependence of ENSO teleconnections over South America and relationships with precipitation in Uruguay, *J. Clim.*, *16*, 1159–1176.

Diaz, A., and P. Aceituno (2003), Atmospheric circulation anomalies during episodes of enhanced and reduced convective cloudiness over Uruguay, *J. Clim.*, *16*, 3171–3185.

Doyle, M., and V. Barros (2002), Midsummer low-level circulation and precipitation in subtropical South America and related sea surface temperature anomalies in the South Atlantic, *J. Clim.*, *15*, 3394–3410.

Grimm, A. M., and P. L. Silva Dias (1995), Analysis of tropical-extratropical interactions with influence functions of a barotropic model, *J. Atmos. Sci.*, *52*, 3538–3555.

Gualdi, S., E. Guilyardi, A. Navarra, S. Masina, and P. Delecluse (2003), The interannual variability in the tropical Indian Ocean as simulated by a CGCM, *Clim. Dyn.*, *20*, 567–582.

Hoskins, B., and D. Karoly (1981), The steady linear response of a spherical atmosphere to thermal and orographic forcing, *J. Atmos. Sci.*, *38*, 1179–1196.

Kalnay, E., et al. (1996), The NCEP/NCAR 40-year reanalysis project, *Bull. Am. Meteorol. Soc.*, *77*, 437–471.

Liebmann, B., G. N. Kiladis, J. A. Marengo, T. Ambrizzi, and J. D. Glick (1999), Submonthly convective variability over South America and the South Atlantic convergence zone, *J. Clim.*, *12*, 1877–1891.

Luo, J. J., S. Masson, S. Behera, P. Delecluse, S. Gualdi, A. Navarra, and T. Yamagata (2003), South Pacific origin of the decadal ENSO-like variations as simulated by a coupled GCM, *Geophys. Res. Lett.*, *30*(24), 2250, doi:10.1029/2003GL018649.

Masson, S., et al. (2004), Impact of barrier layer on winter-spring variability of the southeastern Arabian Sea, *Geophys. Res. Lett.*, *32*, L07703, doi:10.1029/2004GL021980.

Mo, K. C., and J. Nogués-Paegle (2001), The Pacific–South American modes and their downstream effects, *Int. J. Climatol.*, *21*, 1211–1229.

Nogués-Paegle, J., and K. C. Mo (1997), Alternating wet and dry conditions over South America during summer, *Mon. Weather Rev.*, *125*, 279–291.

Nogués-Paegle, J., et al. (2002), Progress in Pan American CLIVAR research: Understanding the South American Monsoon, *Meteorologica*, *27*, 3–30.

Rayner, N. A., P. Brohan, D. E. Parker, C. K. Folland, J. J. Kennedy, M. Vanicek, T. Ansell, and S. F. B. Tett (2006), Improved analyses of changes and uncertainties in marine temperature measured in situ since the mid-nineteenth century: The HadSST2 dataset, *J. Clim.*, *19*, 446–469.

Robertson, A. W., and C. R. Mechoso (2000), Interannual and interdecadal variability of the South Atlantic Convergence Zone, *Mon. Weather Rev.*, *128*, 2947–2957.

Saji, N. H., and T. Yamagata (2003), Possible impacts of Indian Ocean Dipole mode events on global climate, *Clim. Res.*, *25*, 151–169.

Saji, N. H., B. N. Goswami, P. N. Vinayachandran, and T. Yamagata (1999), A dipole mode in the tropical Indian Ocean, *Nature*, *401*, 360–363.

Saji, N. H., T. Ambrizzi, and S. E. T. Ferraz (2005), Indian Ocean Dipole Mode events and austral surface temperature anomalies, *Dyn. Atmos. Oceans*, *39*, 87–102.

Sardeshmukh, P. D., and B. Hoskins (1988), The generation of global rotational flow by steady idealized tropical divergence, *J. Atmos. Sci.*, *45*, 1228–1251.

Silvestri, G. E., and C. S. Vera (2003), Antarctic Oscillation signal on precipitation anomalies over southeastern South America, *Geophys. Res. Lett.*, *30*(21), 2115, doi:10.1029/2003GL018277.

Trenberth, K. E., G. W. Branstator, D. Karoly, A. Kumar, N.-C. Lau, and C. Ropelewski (1998), Progress during TOGA in understanding and modeling global teleconnections associated with tropical sea surface temperatures, *J. Geophys. Res.*, *103*, 14,291–14,324.

Vera, C., et al. (2006), Toward a unified view of the American monsoon systems, *J. Clim.*, *19*, 4977–5000.

Willmott, C. J., and K. Matsuura (1995), Smart interpolation of annually averaged air temperature in the United States, *J. Appl. Meteorol.*, *34*, 2557–2586.

Yamagata, T., S. K. Behera, J.-J. Luo, S. Masson, M. Jury, and S. A. Rao (2004), Coupled ocean-atmosphere variability in the tropical Indian Ocean, in *Earth Climate: The Ocean-Atmosphere Interaction*, *Geophys. Monogr. Ser.*, vol. 147, edited by C. Wang, S.-P. Xie, and J. A. Carton, pp. 189–212, Washington, D.C.

S. K. Behera and T. Yamagata, Frontier Research Center for Global Change/JAMSTEC, Yokohama 236-0001, Japan. (yamagata@eps.s.u-tokyo.ac.jp)

S. C. Chan, Department of Meteorology, University of Maryland, College Park, MD 20742–2425, USA.